

Case Report

DOI: 10.3348/kjr.2011.12.4.519
 pISSN 1229-6929 · eISSN 2005-8330
 Korean J Radiol 2011;12(4):519-523

MRI Appearance of Prostatic Stromal Sarcoma in a Young Adult

Tsutomu Tamada, MD¹, Teruki Sone, MD¹, Yoshiyuki Miyaji, MD², Yuji Kozuka, MD³, Katsuyoshi Ito, MD¹

Departments of ¹Radiology, ²Urology and ³Pathology, Kawasaki Medical School, Okayama 701-0192, Japan

Prostatic stromal sarcoma (PSS) is quite rare. Herein, we describe magnetic resonance imaging (MRI) features of a PSS identified in a 26-year-old man with dysuria and hematuria. MRI clearly depicted the extent and multinodular appearance of the tumor, which was mainly located in the central zone of the prostate. The tumor appeared as a heterogeneously signal-hyperintense mass with a pseudocapsule on T2-weighted imaging. Contrast-enhanced T1-weighted MRI showed necrotic portions in the gradually enhanced solid mass, and diffusion-weighted imaging permitted the accurate assessment of the local extent of the tumor. Thus, the appearance on MRI was quite different from that of adenocarcinoma of the prostate.

Index terms: Prostatic stromal sarcoma; Prostatic neoplasms; Magnetic resonance (MR); Diffusion magnetic resonance imaging; T2-weighted imaging, dynamic contrast-enhanced MRI

INTRODUCTION

Prostatic stromal sarcoma (PSS) is quite rare, comprising only 0.1-0.2% of all malignant prostate tumors (1). In 1998, Gaudin et al. (2) classified sarcoma-related proliferative lesions of the specialized prostatic stroma, including prostatic phyllodes tumors, into two subtypes: prostatic stromal proliferation of uncertain malignant potential and PSS (2, 3). Herein, we present a case of PSS in a young man. To the best of our knowledge, only three reports of PSS with findings from computed tomography (CT) have been reported in the English literature (1, 4,

5). However, none of those reports described findings on magnetic resonance imaging (MRI). This represents the first report in the radiological literature on the MRI appearance of PSS.

CASE REPORT

A 26-year-old man presented with a history of dysuria and hematuria for about one month. A digital rectal examination revealed a huge hard mass with an irregular surface. Serum levels of prostate-specific antigen (PSA) were not elevated (0.44 ng/mL). Various other tumor markers were also within normal limits. MRI was performed using a 1.5-T Signa Excite scanner (GE Medical Systems, Milwaukee, WI) and a phased-array torso coil. T2-weighted fast spin-echo (FSE) imaging in the transverse and coronal planes, T2-weighted echo-planar imaging (EPI) in the transverse plane, T1-weighted FSE imaging in the transverse plane, diffusion-weighted imaging (DWI) (using b-factors of 0 and 800 s/mm²) in the transverse plane, dynamic contrast-enhanced MRI (DCE-MRI) in the transverse plane, and contrast-enhanced T1-weighted FSE imaging in the transverse plane were performed.

Received December 10, 2010; accepted after revision February 16, 2011.

Corresponding author: Tsutomu Tamada, MD, Department of Radiology, Kawasaki Medical School, 577 Matsushima, Kurashiki City, Okayama 701-0192, Japan.

• Tel: (8186) 462-1111 • Fax: (8186) 462-1199

• E-mail: ttamada@med.kawasaki-m.ac.jp

This is an Open Access article distributed under the terms of the Creative Commons Attribution Non-Commercial License (<http://creativecommons.org/licenses/by-nc/3.0>) which permits unrestricted non-commercial use, distribution, and reproduction in any medium, provided the original work is properly cited.

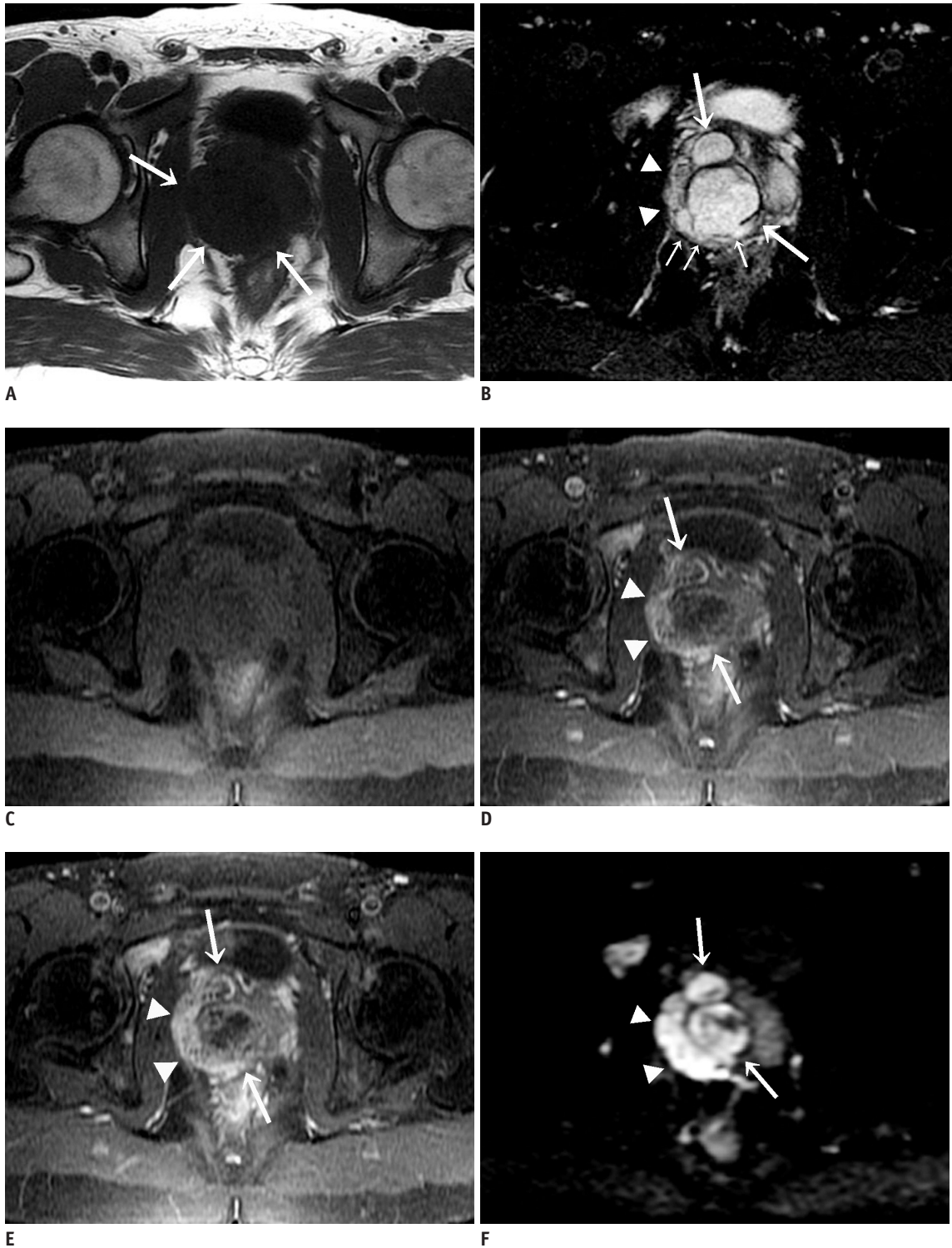


Fig. 1. Prostatic stromal sarcoma in 26-year-old man.

A. Axial T1-weighted image showing mass located centrally and to right side of prostate with homogeneous slight low signal intensity in comparison with left side of prostate (arrows). **B.** Axial T2-weighted echo-planar image showing multinodular mass (arrows) with irregular margins associated with nodular lesions (small arrows) in posterior part of mass, and presenting heterogeneous high signal intensity. Right peripheral gland (arrowheads) is compressed by central glandular mass. **C-E.** Axial dynamic contrast-enhanced MR images at 0 s (**C**), 30 s (**D**) and 150 s (**E**) after contrast injection, showing weakly enhanced mass containing non-enhanced cystic areas in central gland (arrows). As right peripheral gland shows gradual moderate enhancement (arrowheads), which differs from enhancement in left peripheral gland, tumor invasion to right peripheral gland is suggested. **F.** Axial diffusion-weighted image showing central gland mass (arrows) and right peripheral zone mass (arrowheads) as areas of marked high signal intensity.

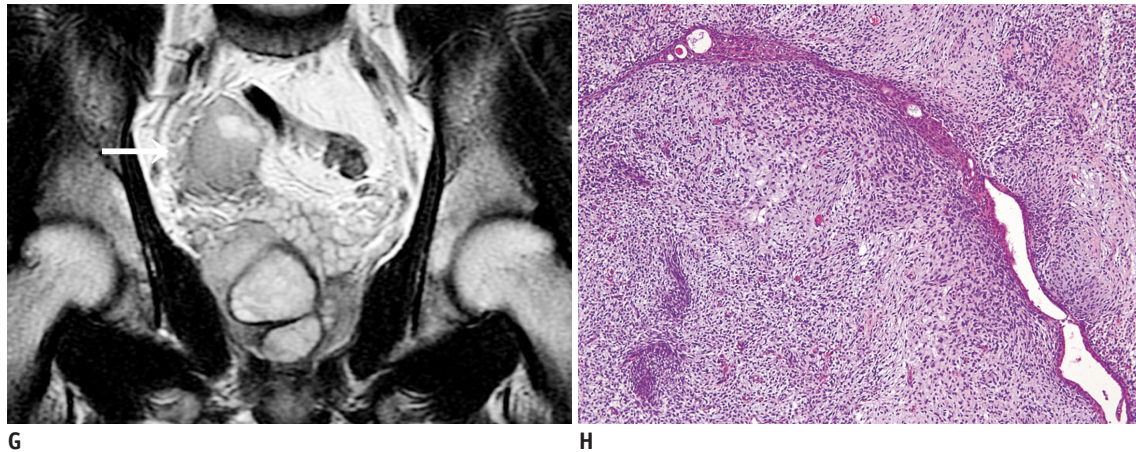


Fig. 1. Prostatic stromal sarcoma in 26-year-old man.

G. Coronal T2-weighted image showing markedly enlarged lymph nodes near seminal vesicle and separated from prostatic mass (arrow). **H.** Histological findings from transurethral resection of prostate. Low-power views show leaf-like projection of proliferating stroma. Cellular stroma contains round and spindle-shaped cells with atypia and mitosis (Hematoxylin & Eosin staining, $\times 100$).

Data acquisition for DCE-MRI began simultaneously with the initiation of intravenous injection of gadopentetate dimeglumine (Magnevist; Bayer Schering Pharma, Osaka, Japan) at 0.1 mmol/kg body weight within 10 s through a peripheral intravenous cannula. This was followed by a 40-mL flush with saline. Multiphase DCE images (6 phases) were obtained every 30 s for 150 s without breath-holding.

MRI revealed an uneven multinodular mass located mainly within the central zone of the prostate and extending to the right peripheral gland at the bottom level of the central gland mass. The mass showed homogeneous low signal intensity on T1-weighted imaging (Fig. 1A) and heterogeneous high signal intensity with pseudocapsule on T2-weighted EPI (Fig. 1B). In DCE-MRI, the central gland portion of the mass showed a weak gradual enhancement containing cystic areas, whereas the right peripheral gland showed a moderate gradual enhancement (Fig. 1C-E). DWI showed the prostatic mass as an area of marked high signal intensity (Fig. 1F). Coronal T2-weighted imaging demonstrated enlarged internal iliac lymph nodes (Fig. 1G).

Transrectal ultrasonography-guided prostate biopsy and transurethral resection of prostate were performed. The resected specimen predominantly comprised elongated ducts and cellular stroma that contained areas of necrosis with calcification (Fig. 1H). Hypercellular stroma without glands was specifically detected. Although epithelial components did not show malignant changes, stromal cells showed ovoid, spindle-shaped and hyperchromatic nuclei in cellular areas, and spindle-shaped nuclei in myxomatous areas. An average of two mitoses per high-powered field was counted. Epithelial cells showed positive immunostaining

for pan-cytokeratin (AE1/AE3, CAM5.2). In stromal cells, positive immunostaining was detected for vimentin, CD34, and progesterone receptor; whereas, negative results were obtained for pan-cytokeratin, CD31, S-100, HHF-35, desmin, α smooth muscle actin, MyoD1, c-kit, and estrogen receptors. The MIB-1 labeling index was elevated to $> 50\%$. Consequently, the tumor was histologically diagnosed as PSS (2).

Although the patient was treated by chemotherapy, he showed progressive disease with bone, lung, liver, and mediastinal lymph node metastases and died seven months after admission.

DISCUSSION

Primary prostate sarcomas are rare malignant tumors of the prostate gland (1, 2). Leiomyosarcoma is the most common histological subtype of prostate sarcoma seen in adults (6). Prostate stromal sarcoma is rarer with fewer than 30 documented cases (1-5, 7-16). Most patients with prostatic sarcoma, including PSS, present with symptoms of urethral obstruction (1-3, 5, 6), as in the present case. The mass effect of the tumor, mainly located in the central gland, probably caused the early onset of symptoms (17). In previous reports on PSS, age at diagnosis has ranged from 19 to 86 years (mean, 48 years) (1-5, 7-16). PSA levels in patients with PSS including the present case have been relatively low (0.1-4.5 ng/mL) in comparison with prostatic adenocarcinoma (1, 3-5). PSS is often large, with most tumors having a diameter > 4 cm (1, 3-5). In immunohistochemical studies, PSS are typically positive for

vimentin and CD 34, and negative for estrogen receptor and HHF-35 (1, 2).

On MRI, a prostatic adenocarcinoma typically demonstrates an unidentified area with signal isointensity relative to background prostatic structures on T1-weighted imaging; an area in the peripheral zone with homogeneous low signal intensity with mass effect, or an area in the transition zone with homogeneous low signal intensity, ill-defined margins, and lack of a capsule, with or without a lenticular shape and invasion of anterior fibromuscular stroma on T2-weighted imaging; an area with focal early enhancement on DCE-MRI; and an area with focal high signal intensity relative to background prostatic structures on DWI (18-21). In the present case, the main tumor in the central gland showed a multinodular shape with heterogeneous high signal intensity and a low signal intensity pseudocapsule on T2-weighted imaging. Furthermore, both areas of tumor showed gradual weak enhancement on DCE-MRI. PSS may differ from a typical adenocarcinoma with respect to shape, vascularity on DCE-MRI, and signal intensity on T2-weighted imaging, thus reflecting tissue construction and cellular structure. Conversely, these PSS findings resemble those of leiomyosarcoma and rhabdomyosarcoma, which are a more common form of sarcoma involving the prostate (22, 23). Furthermore, DWI clearly demonstrated both central gland and peripheral zone parts of the tumor as showing marked high signal intensity, suggesting the usefulness of this modality for determining the local extent of the lesion. MRI features of PSS have not previously been reported in the English literature. However, two reports of MRI findings for stromal sarcoma of uterine endometrium by Koyama et al. (24) and Ueda et al. (25) demonstrated that stromal sarcoma was relatively large and showed heterogeneous signal intensity on T2-weighted imaging, heterogeneous contrast enhancement of the tumor, marginal nodules, multiple nodule formation, hemorrhage, and necrosis in the tumor. All these MRI findings except hemorrhage were also seen in our case.

MRI findings including T2-weighted imaging, DCE-MRI, and DWI in the present case seemed to reflect the pathological features of PSS, which include aggressive tumor growth, greater cellularity, and necrosis with mitotic activity.

In the present case, the tumor was mainly located in the central gland, and appeared as a signal hypointense mass on T1-weighted imaging, and as a heterogeneously signal hyperintense multinodular mass on T2-weighted imaging.

DCE-MRI indicated weak to moderate gradual enhancement containing cystic areas. PSS did not resemble prostatic adenocarcinoma on MRI, which may thus play a role in differentiating PSS from prostatic adenocarcinoma. When an adult male shows MRI findings as mentioned above, although these imaging findings are not pathognomonic, PSS should be included in the differential diagnoses of a prostatic adenocarcinoma.

REFERENCES

1. Chang YS, Chuang CK, Ng KF, Liao SK. Prostatic stromal sarcoma in a young adult: a case report. *Arch Androl* 2005;51:419-424
2. Gaudin PB, Rosai J, Epstein JI. Sarcomas and related proliferative lesions of specialized prostatic stroma: a clinicopathologic study of 22 cases. *Am J Surg Pathol* 1998;22:148-162
3. Morikawa T, Goto A, Tomita K, Tsurumaki Y, Ota S, Kitamura T, et al. Recurrent prostatic stromal sarcoma with massive high-grade prostatic intraepithelial neoplasia. *J Clin Pathol* 2007;60:330-332
4. Probert JL, O'Rourke JS, Farrow R, Cox P. Stromal sarcoma of the prostate. *Eur J Surg Oncol* 2000;26:100-101
5. Huang YC, Wang JY, Lin PY, Chin CC, Chen CS. Synchronous prostate stromal sarcoma and gastrointestinal stromal tumor of rectum: case report and review of the literature. *Urology* 2006;68:672 e611-673
6. Sexton WJ, Lance RE, Reyes AO, Pisters PW, Tu SM, Pisters LL. Adult prostate sarcoma: the M. D. Anderson Cancer Center Experience. *J Urol* 2001;166:521-525
7. Colombo P, Ceresoli GL, Boiocchi L, Taverna G, Grizzi F, Bertuzzi A, et al. Prostatic stromal tumor with fatal outcome in a young man: histopathological and immunohistochemical case presentation. *Rare Tumors* 2010;2:e57
8. Kim JY, Cho YM, Ro JY. Prostatic stromal sarcoma with rhabdoid features. *Ann Diagn Pathol* 2010;14:453-456
9. Frassetta F, Pepe P, Giunta ML, Aragona F. Primary high grade sarcoma of the specialised prostatic stroma: a case report with clinico-pathological considerations. *Pathologica* 2008;100:482-484
10. Herawi M, Epstein JI. Specialized stromal tumors of the prostate: a clinicopathologic study of 50 cases. *Am J Surg Pathol* 2006;30:694-704
11. Bostwick DG, Hossain D, Qian J, Neumann RM, Yang P, Young RH, et al. Phyllodes tumor of the prostate: long-term followup study of 23 cases. *J Urol* 2004;172:894-899
12. Malhotra P, Bhatia A, Arora VK, Singh N. Pathologic quiz case: a 70-year-old man with bladder outflow obstruction. Prostatic stromal sarcoma. *Arch Pathol Lab Med* 2004;128:e81-82
13. Osaki M, Takahashi C, Miyagawa T, Adachi H, Ito H. Prostatic stromal sarcoma: case report and review of the literature. *Pathol Int* 2003;53:407-411

14. Froehner M, Bartholdt E, Meye A, Manseck A, Wirth MP. Adult prostate sarcoma diagnosed from tissue spontaneously excreted through the urethra. *Urol Oncol* 2004;22:119-120
15. Sakura M, Tsukamoto T, Yonese J, Ishikawa Y, Aoki N, Fukui I. Successful therapy of a malignant phyllodes tumor of the prostate after postoperative local failure. *Urology* 2006;67:845 e811-843
16. De Raeve H, Jeuris W, Wyndaele JJ, Van Marck E. Cystosarcoma phyllodes of the prostate with rhabdomyoblastic differentiation. *Pathol Res Pract* 2001;197:657-662
17. Cheng YC, Wang JH, Shen SH, Chang YH, Chen PC, Pan CC, et al. MRI findings of prostatic synovial sarcoma. *Br J Radiol* 2007;80:e15-18
18. Bezzi M, Kressel HY, Allen KS, Schiebler ML, Altman HG, Wein AJ, et al. Prostatic carcinoma: staging with MR imaging at 1.5 T. *Radiology* 1988;169:339-346
19. Tamada T, Sone T, Nagai K, Jo Y, Gyoten M, Imai S, et al. T2-weighted MR imaging of prostate cancer: multishot echo-planar imaging vs fast spin-echo imaging. *Eur Radiol* 2004;14:318-325
20. Akin O, Sala E, Moskowitz CS, Kuroiwa K, Ishill NM, Pucar D, et al. Transition zone prostate cancers: features, detection, localization, and staging at endorectal MR imaging. *Radiology* 2006;239:784-792
21. Tamada T, Sone T, Jo Y, Yamamoto A, Yamashita T, Egashira N, et al. Prostate cancer: relationships between postbiopsy hemorrhage and tumor detectability at MR diagnosis. *Radiology* 2008;248:531-539
22. Bartolozzi C, Selli C, Olmastroni M, Menchi I, Di Candio G. Rhabdomyosarcoma of the prostate: MR findings. *AJR Am J Roentgenol* 1988;150:1333-1334
23. Chang JM, Lee HJ, Lee SE, Byun SS, Choe GY, Kim SH, et al. Pictorial review: Unusual tumours involving the prostate: radiological-pathological findings. *Br J Radiol* 2008;81:907-915
24. Koyama T, Togashi K, Konishi I, Kobayashi H, Ueda H, Kataoka ML, et al. MR imaging of endometrial stromal sarcoma: correlation with pathologic findings. *AJR Am J Roentgenol* 1999;173:767-772
25. Ueda M, Otsuka M, Hatakenaka M, Sakai S, Ono M, Yoshimitsu K, et al. MR imaging findings of uterine endometrial stromal sarcoma: differentiation from endometrial carcinoma. *Eur Radiol* 2001;11:28-33